Received: 3 August 2021 | Revised: 30 August 2021 | Accepted: 2 September 2021

DOI: 10.1002/pat.5507

RESEARCH ARTICLE

polymers advanced technologies WILEY

# Rational design of salmeterol xinafoate imprinted polymer through computational method: Functional monomer and crosslinker selection

Shendi Suryana[1,2] | Mutakin Mutakin[1] | Yudi Rosandi[3] | Aliya Nur Hasanah[1,4]

[1]Department of Pharmaceutical Analysis and Medicinal Chemistry, Faculty of Pharmacy, Universitas Padjadjaran, Sumedang, Indonesia

[2]Department of Pharmacy, Faculty of Mathematics and Natural Sciences, Universitas Garut, Garut, Indonesia

[3]Geophysic Department, Faculty of Mathematics and Natural Sciences, Universitas Padjadjaran, Sumedang, Indonesia

[4]Drug Development Study Center, Faculty of Pharmacy, Universitas Padjadjaran, Sumedang, Indonesia

**Correspondence**
Aliya Nur Hasanah, Drug Development Study Center, Faculty of Pharmacy, Universitas Padjadjaran, Jl. Raya Bandung Sumedang KM 21,5 Jatinangor, Sumedang, Indonesia.
Email: aliya.n.hasanah@unpad.ac.id

**Funding information**
Directorate General of Higher Education, Ministry of Education and Culture Indonesia

## Abstract

A molecular imprinted polymer (MIP) was computationally designed and synthesized for the selective extraction of salmeterol xinafoate (SLX) from human serum. In this study, semi-empirical PM3 calculations were used to find a suitable functional monomer (FM), the ratio of template (T) to FM, and types of crosslinkers. MIPs were synthesized with 2-hydroxyethyl methacrylate (HEMA) with T:FM mol ratios of 1:6 and 1:4 and ethylene glycol dimethacrylate (EGDMA) or trimethylolpropane trimethacrylate (TRIM) as a crosslinker. On the basis of computational and experimental results, HEMA and TRIM in the mol ratio 1:6 of T-FM (MIP3) were found to be the best choices of FM and crosslinker, respectively. These polymers were then used as a selective sorbent to develop a molecularly imprinted solid-phase extraction procedure followed by high performance liquid chromatography with UV detection for the determination of SLX in serum. The extraction ability of MIP3 was excellent with a recovery of 92.17% ± 2.66% of SLX in spiked serum, and 91.15% ± 1.12% when SLX was spiked as a mixture with another analogous structure. By comparing the performance of the synthesized sorbent with a C-18 cartridge with a recovery of 79.11% ± 2.96%, it was determined that MIP had better performance over the latter. On the basis of these results, the imprinted receptor MIPs, especially MIP 3, can be applied for the direct extraction of SLX in clinical analysis.

KEYWORDS

computational design, molecularly imprinted polymers, salmeterol xinafoate, solid-phase extraction

## 1 | INTRODUCTION

Salmeterol xinafoate (SLX) is a long-acting beta adrenergic receptor agonist whose function is to control long-term asthma with an indication for its use as an adjunct drug therapy for patients already receiving corticosteroids.[1,2] At doses of more than 200 μg, salmeterol can increase the risk of death related to asthma because of the paradoxical bronchospasm Besides that, salmeterol has various side effects–namely cardiovascular disorders, seizures, thyrotoxicity, risk of hypocalcemia, and increased serum glucose, so caution must be given to patients with diabetes mellitus.[3] Like other β-2 agonists, Salmeterol is prohibited from being used in sports by the World Anti-Doping Agency (WADA) because it can increase anabolic performance, resulting in increased stamina.[4] However, in athletes who also suffer from asthma, the use of salmeterol is still allowed with a maximum dose of 200 μg.[5] The sample preparation used for salmeterol analysis in blood samples includes liquid–liquid extraction (LLE)[6] and solid phase extraction (SPE),[7] whereas the urine sample includes LLE[5] and enzymatic hydrolysis followed by LLE.[4] Sample preparation, which aims to isolate the target analyte from various complex sample

  

matrices, is an important step in the analysis.[8] Sample preparation also aims to concentrate the target analyte, which is in low concentrations and in the form of mixtures with other compounds that have similar physicochemical properties, so that it can be easily measured.[9] SPE is the most common sample preparation technique; it has been introduced in place of LLE.[10] Its main advantages are better selectivity and use of a smaller volume of solvent.[11] The molecular imprinting polymer is a technique for making SPE to increase the selectivity of conventional SPE.[8,12] An adsorbent based on a molecularly imprinted polymer (MIP) can increase sample selectivity and make it easier for samples to be analyzed.[13]

An MIP is a polymer that has a special affinity for a target molecule after removal of the template molecule. The cavity is able to recognize the target molecule with the same structure and properties as the template molecule.[14] MIP synthesis is based on the principle of polymerization which combines functional monomers (FM), crosslinker, initiator, and porogen solvents.[15] The MIP synthesis process requires optimal selection of the right FM and solvent[16] and the appropriate ratio of template molecules and FMs.[17] Apart from that, another component in an MIP, namely the crosslinker, also plays an important role in making an MIP.[18] The crosslinker will keep the functional groups of the FMs in position and will surround the template molecule and maintain the structure of the binding site.[19] Therefore the molecular recognition ability of MIP and its chemical and physical properties are highly dependent on the degree of crosslinking and the properties of the crosslinker used.[20]

The best method for optimizing MIP synthesis is to use a computational approach because the calculation is easy, the cost is low, the processing time is short, it is safe for health, there is no waste, and many variables can be optimized directly.[21–25] A computational approach is used to obtain imprinting effectiveness by calculating the template molecules and FMs. The results of the computational approach are important in MIP preparation in order to obtain high selectivity.[26] To the base of our knowledge, until now, no MIP on SLX has been developed. Based on this, this study carried out to develop MIP for SLX using a computational approach to screen for a FM with the best interaction with the template molecule as well as a screening for the crosslinker that would be most appropriate for use in the synthesis of MIP salmeterol. The results of the computational approach then used in the basis for the synthesis of MIP SLX. MIP that synthesized then used to analyzed salmeterol from biological fluids by comparing the result with SPE C-18 cartridge.

## 2 | EXPERIMENTAL

### 2.1 | Materials and methods

SLX, terbutaline (TER), and salbutamol (SAL) were purchased from Tokyo Chemical Industry, hydroxy ethyl methacrylate (HEMA), ethylene glycol dimethacrylate (EGDMA), trimethylol propane trimethacrylate (TRIM), and benzoyl peroxide (BPO) were obtained from Sigma Aldrich (Singapore). HPLC grade methanol, isopropanol, and acetonitrile were purchased from Fischer Scientific. Acetic acid was purchased from Merck. Blood samples were provided by the Indonesian Red Cross. Empty SPE cartridges were purchased from Supelco. C-18 cartridges were purchased from Chromabond. If not otherwise specified, all chemicals are analytical grade. A computer with a 2.0 GHz Intel® Core TM i3-5005U processor, 8 GB DDR3 RAM memory, and a Windows 10 operating system was used for the computational method. Hyperchem 8.0.7 software was used to optimize the geometry of molecules and for binding site prediction and calculation of binding energy. The morphological evaluation analysis was carried out by JSM-6610LV JEOL Ltd. The surface area of sorbent beads were analyzed using a multipoint Brunauer–Emmett–Teller (BET) apparatus (Nova 2200E, Quantachrome, Boynton Beach, FL, United States). A UV–visible spectrophotometer (Shimadzu) was used to detect the UV absorbance for constant association determination. Analyses of blood after extraction with the MI-SPE were performed using HPLC (Waters Alliance e2695 with a UV detector) by gradient elution, using a mixture of water/acetonitrile containing the mobile phase and a Zorbax Eclipse XDB-C18 column (4.6 × 150mm, 5 μm). The injection volume was 20 μl with a constant flow rate of 0.8 ml $min^{-1}$ and the detection wavelength was set at 252 nm. IR analysis was carried out with a Nicolet 380 FT-IR. An SPE manifold was purchased from Phenomenex.

### 2.2 | Computational selection of FMs

The 3D structures of the template and FMs were drawn using the Hyperchem 8.0.7 program. The molecular structure was optimized using the semi-empirical restricted Hartree–Fock (RHF) method based on the molecular orbital theory. To interact at a suitable position, the electronic data of the SLX molecules represented by contour maps of total charge density and electrostatic potential are presented. The template-FMs complexes were optimized using the PM3 method with self-consistent field (SCF) at the RHF level. All FM selection calculations were referred to as isolated molecules in the gas phase. The gradient conjugate process (Polak–Ribier) was used to optimize the geometry of the molecule using a convergence set at a value of 0.01 Kcal.

The binding energy ($\Delta E$) during the formation of the complex was calculated by the following equation:

$$\Delta E = E_{\text{complexes}} - E_{\text{salmeterol xinafoate}} - (n)E_{\text{functional monomer}} \quad (1)$$

### 2.3 | Computational selection of crosslinker

The 3D structures of the template and crosslinker were drawn using the Hyperchem 8.0.7 program. The molecular structure was optimized using the semi-empirical RHF method based on the molecular orbital theory. The template-FM complexes were optimized using the PM3 method with SCF at the RHF level. All crosslinker selection

calculations referred to isolated molecules in the gas phase. The gradient conjugate process (Polak–Ribier) was used to optimize the geometry of the molecule using a convergence set at a value of 0.01 Kcal .

The binding energy ($\Delta E$) during the formation of the complex was calculated by the following equation:

$$\Delta E = E_{\text{complexes}} - E_{\text{salmeterol xinafoate}} - E_{\text{crosslinker}} \quad (2)$$

## 2.4 | Determination of the association constant for the template-FM with UV–visible spectrophotometry

Monomer-template interaction was studied before polymer synthesis using UV titration to verify the computational method result. To a solution of SLX 0.001 mol $L^{-1}$ in methanol or methanol: isopropanol 1:1, an increasing amount of FM was added until a 10-fold excess was reached. Subsequently, the absorbance was measured. Finally, a curve of the delta absorbance against the monomer concentration was constructed to determine the value of the association constant.

## 2.5 | Stoichiometry reaction analysis (Jobs plot)

A molar ratio plot was constructed by the systematic variation of the molar fraction ratio of SLX and HEMA in a mixture of isopropanol-methanol (1:1). The initial values of SLX and HEMA were 0.002 and 0.01 M, respectively. The total volume was 3 ml, and all absorbances were recorded at 235 nm, then the delta of absorbance was plotted against the molar fraction of SLX.

## 2.6 | Preparation of the MIP and NIP

Two MIPs synthesized using different ratios of template and FM, two MIPs using different crosslinkers, and a total of four MIPs were synthesized through bulk polymerization. The MIP was obtained by dissolving SLX (0.25 mmol) as a template and HEMA as FM (1.5 mmol of HEMA for MIP1 and MIP 3, 1 mmol of HEMA for MIP 2 and MIP 4) in 5 ml of a mixture methanol-isopropanol (1:1) in a closed vial and then sonicating for 5 min. Subsequently, either EGDMA or TRIM (5 mmol) was added to the solution as a crosslinker, followed by sonicating for 40 min. Then benzoyl peroxide (0.206 mmol) was added to the vial as initiator, and finally the vial was placed in an oven at 70°C for 18 h. The resulting bulk polymers were ground and sieved (60 mesh), washed with 20 ml methanol, and dried at 50°C. The non-imprinted polymer (NIP) was prepared simultaneously under the same conditions without the addition of a template. A sonication was used for template removal from the synthesized MIP using methanol and acetic acid (9:1) for 3 h. Then, the polymers were washed using 20 ml of methanol and water and dried at 50°C for 18 h. The MIP was monitored using 20 mg of the MIP diluted in 5 ml of methanol, performed in triplicate. The extraction process was complete when MIP no longer contained the template when monitored using UV–Vis spectrophotometry. The compositions of each of the MIPs and NIPs are shown in Table 1.

## 2.7 | Adsorption capacity evaluation

To evaluate the adsorption capacity, we varied the concentration of the SLX solution, that is, 2.5, 5, 7.5, 10, and 12.5 mg $L^{-1}$. A 5 ml SLX solution was introduced into a vial containing 20 mg of MIP sorbent, then shaken using a shaker at 120 rpm for 3 h at room temperature. Next, the mixture was filtered, and the absorbance of the filtrate was measured using a HPLC. NIP sorbents were treated in the same way as MIP. The results of MIP-SPE adsorption capacity were plotted on the Langmuir and Freundlich isotherm adsorption curves.

## 2.8 | Optimization of the molecularly imprinted SPE condition

Empty plastic SPE cartridges were used for this study. A 200 mg weight of the dry polymer was placed into the cartridges with frits at either end. These were called molecularly imprinted solid-phase extraction (MISPE) and NISPE. Optimization conditions were evaluated to determine the conditioning solvent, the loading solvent, washing, and the elution solvent that resulted in the highest SLX recovery. The effect of concentration on the percent recovery of SLX from the standard solution was also carried out after obtaining the optimum

**TABLE 1** Composition of synthesized MIP and NIP

| Polymer | Template (T) | Functional monomer (FM) | Crosslinker (Cl) | Ratio T:FM:Cl (mmol) |
|---|---|---|---|---|
| MIP 1 | SLX | HEMA | EGDMA | 1:6:20 |
| NIP 1 | - | HEMA | EGDMA | 1:6:20 |
| MIP 2 | SLX | HEMA | EGDMA | 1:4:20 |
| NIP 2 | - | HEMA | EGDMA | 1:4:20 |
| MIP 3 | SLX | HEMA | TRIM | 1:6:20 |
| NIP 3 | - | HEMA | TRIM | 1:6:20 |
| MIP 4 | SLX | HEMA | TRIM | 1:4:20 |
| NIP 4 | - | HEMA | TRIM | 1:4:20 |

Abbreviations: MIP, molecular imprinted polymer; NIP, non-imprinted polymer.

conditions for the washing and eluting solvents. Testing the effect of concentration on the percent recovery of SLX from standard solutions was carried out using SLX in various concentrations ranging from 0.1 to 4 mg $L^{-1}$ (in two different solvents) which was then passed into MISPE and NISPE sorbents.

### 2.9 | Application of polymer to extract SLX from spiked serum, selectivity testing, and comparison with a C-18 cartridge

The blood serum was obtained by centrifugation of the blood at a speed of 5000 rpm for 5 min in 14°C. Then, the upper part was taken. The blood serum was spiked with 2 mg $L^{-1}$ SLX in isopropanol or deionized water. The spiked serum was passed through the MISPE sorbent and the NISPE sorbent. The SPE system used was the best condition determined in Section 2.8. The elution results were then analyzed by HPLC. The serum was spiked with another analogue of SLX, namely TER and SAL. The optimum SPE system conditions were applied, and the percent recovery was calculated for each compound. Extraction of spiked serum with a C-18 cartridge used the method of Grag et al.[27]

### 2.10 | Fourier transform infra-red, scanning electron microscope, and Brunauer–Emmett–Teller measurement of MIP

A Fourier transform infra-red (FTIR) spectrometer and a scanning electron microscope (SEM) were used to see the properties of MIP. A total of 2 mg of MIP sorbent was crushed together with 200 mg of potassium bromide (KBr) then formed into pellets. The infrared spectra of MIP sorbents were observed using FTIR instruments. The transmission was measured at wave numbers 4000–400 $cm^{-1}$. MIP sorbent functional groups were determined after extraction. The surface morphologies of the polymers were observed using SEM by placing MIP and NIP on silicon and then putting them in the SEM instrument. The specific surface area of MIPs was determined using a multipoint BET apparatus. In the BET method, the specific surface area of the beads is related to the amount of $N_2$ gas absorbed on the surface of the beads. 0.5 g of the beads of interest was placed in a sample holder and degassed in a stream of $N_2$ gas at 150°C for 1 h. The adsorption of the $N_2$ gas was conducted at −210°C, while its desorption was performed at room temperature. The instrumental values obtained in the desorption step were used to compute the specific surface area of the beads. NIP sorbents were characterized in the same way using FTIR, SEM, and BET.

## 3 | RESULTS AND DISCUSSION

### 3.1 | Computational selection of FMs

In this study, the interaction analysis of each FM on the SLX template molecules was carried out by calculating the value of the binding energy and studying the non-covalent bonds, especially the hydrogen bonds in the complexes that were formed. First, to interact at a suitable position, the electronic data of the SLX molecules, represented by a contour map of total charge density and electrostatic potential were examined. The contour of the electrostatic potential can then be used to predict which areas of interaction that will happened between FMs and templates.[28] The amine group is an electron withdrawing group, and the presence of N and O groups which are the electronegative centers in the system act as electron-attracting groups. Meanwhile, the xinafoate structure of the biphenyl group has hydroxyl and carboxylate group substituents that act as the electron donating groups.[29] The main consideration in MIP synthesis is the formation of a stable complex which is expressed by the low energy of the SLX–FM interaction.[30] To find the best FM interaction with SLX, the template-FM complexes were optimized using the PM3 method with SCF at RHF level. The PM3 method was chosen because it is very fast, applicable to large molecules and give accurate result for simulating intra- and intermolecular interactions.[25] The binding energy ($\Delta E$) during the formation of the complexes were then calculated. Table 1 shows the binding energy value results between template (SLX) and eight FMs that are generally used in making imprinted polymers.

The binding energy data shows the stability of the complex formed. The lower the value of the binding energy, indicated by the negative $\Delta E$ value, the more likely the complex formed will exist in its complex form.[31] In other words, a complex with a low $\Delta E$ value will be able to provide better selectivity to the synthesized MIP. The three complexes with the lowest interaction energy were formed from the SLX structure and the FMs HEMA, 4-VBA, and 4-VP with energies of −29.37, −26.09, and −23.08 kcal $mol^{-1}$ respectively. This low interaction energy value indicates that the MIP formed using these three FMs will provide excellent MIP selectivity compared to other complexes. The number of FMs interacting with the template shows the stoichiometry of the reaction, and this was used for the mol ratio of T:FM in synthesizing the polymers. The illustration of the interaction between SLX and the three best FMs is shown in Figure 1.

In the process of selecting FMs that are effective for MIP synthesis, the formation of hydrogen bonds in the complex of FM-template is a very important. Hydrogen bonding produces better interaction sites. A larger number of hydrogen bonds formed will produce an MIP with higher affinity and selectivity.[32] The number of FMs in the complex formed between the template and the FM showed the maximum of number of hydrogen bonds that effect the ratio of T-FM used to synthesize polymer. The simulation founded six HEMA will formed stable complex with lowest binding energy with one SLX (Table 2). This result will be confirmed by stoichiometric determination using Job's plot.

### 3.2 | Computational crosslinker selection

Crosslinkers have the role of securing the functional groups of FMs in specific locations and directions around template molecules and thereby preserving the structure of the binding site (cavity).[33] The

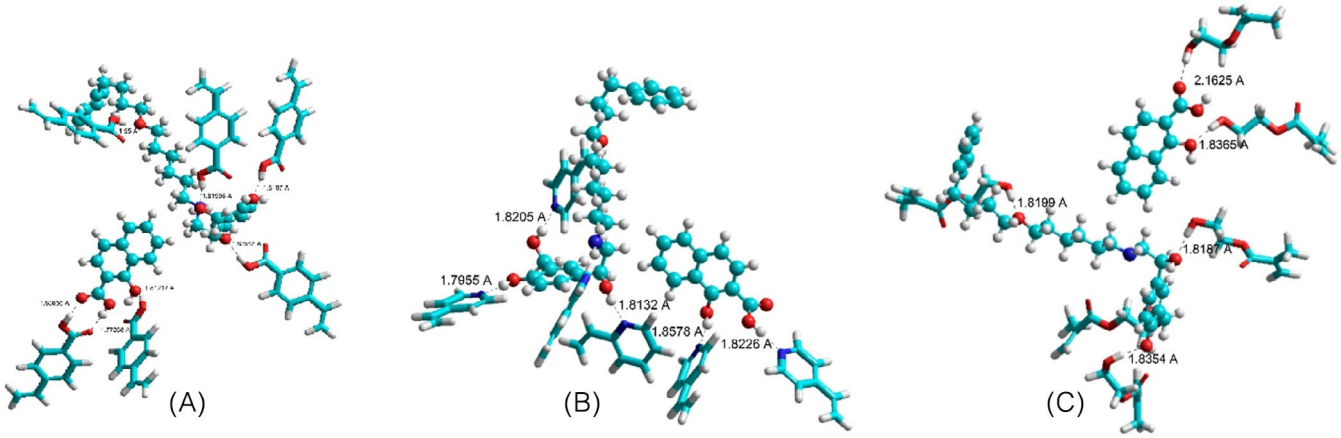


**FIGURE 1** Illustrations of interactions between salmeterol xinafoate and functional monomers: (A) 4-VBA, (B) 4-VP, and (C) HEMA

**TABLE 2** Binding energy ($\Delta E$) of salmeterol xinafoate-functional monomer complex

| Functional monomer | $\Delta E$ (Kcal mol$^{-1}$) | Number functional monomer interactions with template through hydrogen bonding |
|---|---|---|
| 2-Hydroxylethylmethacrylate (HEMA) | −293,776,493 | 6 |
| 4-Vinyl pyridine (4-VP) | −26,095,754 | 6 |
| 4-Vinyl benzoic acid (4-VBA) | −230,871,442 | 6 |
| Acrylamide (AAM) | −22,444,608 | 4 |
| Methacrylic acid (MAA) | −222,811,154 | 6 |
| 2-Fluorometyl acrylic acid (TFMAA) | −21,095,754 | 5 |
| Methacrylamide (MCA) | −182,635,128 | 6 |
| Acrylic acid (AA) | −133,676,338 | 5 |

crosslinker should not interfere with the interaction of T-FM complexes because this can reduce the selectivity of the synthesized polymer.[34] Crosslinker screening was carried out for ethylene glycol dimethacrylate (EGDMA), trimethylolpropane trimethacrylate (TRIM), and divinylbenzene (DVB) to obtain the crosslinker with the highest bond energy. A template-crosslinker complex with a weaker interaction than template-FMs will increase the selectivity of the resulting polymer.[33]

From the results in Table 3, TRIM has much higher energies (−5.9829774 kcal mol$^{-1}$) compared to the other two crosslinkers. It is possible to suggest that TRIM would be considered to be the best crosslinker for an imprinted SLX molecule because it has weaker interaction with template thus would not bind to it. Two other crosslinkers, especially DVB, will have a competition with FMs binding to the template, and this will affect the formation of imprinted polymer which

**TABLE 3** Binding energy ($\Delta E$) result between template-crosslinker

| No | Crosslinker | $\Delta E$ (Kcal mol$^{-1}$) |
|---|---|---|
| 1 | EGDMA | −10.7143115 |
| 2 | TRIM | −5.9829774 |
| 3 | DVB | −17.6703403 |

will affect its analytical performance latter. An illustration of the interactions between SLX and three kinds of crosslinkers is depicted in Figure 2.

### 3.3 | Determination of the association constant for the template-FM with UV–visible spectrophotometry

Determination of the association constants between template-FM were done by using UV titration. HEMA was used as the FM that was studied, according to the results from the computational method. The association constant ($K_a$) values are associated with the binding affinity of a FM to the template. On calculating Ka values of SLX-HEMA, increasing amounts of FMs were added to a solution of SLX (0.001 mol L$^{-1}$) in two kinds of solvents, methanol and a solvent mixture (methanol: isopropanol, 1:1), until at least a 10-fold excess was reached. At this point, delta absorbance was recorded, and the results were plotted on the curve. The association constant was calculated based on the slope value and the graph intercept using the Benesi–Hildebrand equation. As seen in Table 4, the association constant of the SLX-HEMA complex was higher in the mixture of methanol-isopropanol (1:1) than in methanol. This result is due to the lower dielectric constant ($K_d$) value of the mixture (21.38) than methanol (24.86). A less polar solvent provides a strong interaction between the template and the FM through hydrogen bonding.[35] The methanol: isopropanol mixture was then used as the porogenic solvent in further MIP and NIP synthesis.

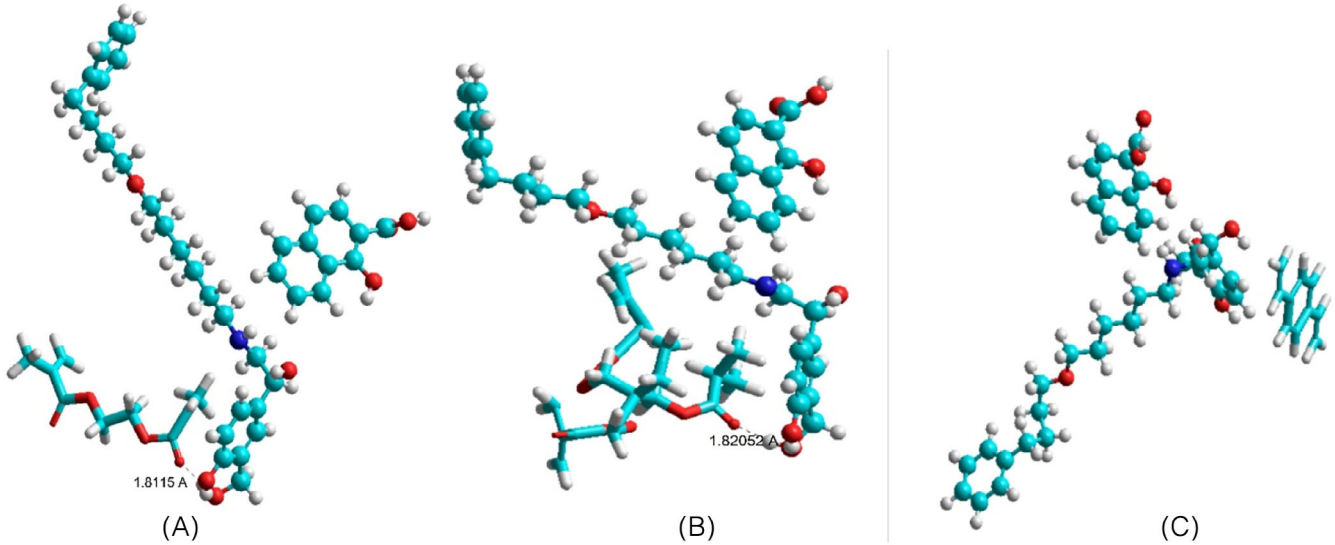


**FIGURE 2** Illustrations of interactions between SLX and crosslinkers: (A) EGDMA, (B) TRIM, and (C) DVB

**TABLE 4** Association constant results of HEMA–SLX on different solvent

| Monomer | Solvent | Template | Ka ($M^{-1}$) |
|---|---|---|---|
| HEMA | Methanol | SLX | $2.62 \times 10^2$ |
| | Methanol: isopropanol (1:1) | SLX | $1.4 \times 10^3$ |

## 3.4 | Stoichiometry reaction analysis (Jobs plot)

In the Jobs method, a series of mixed solutions of template (T) and FMs are prepared such that the total concentration [T] + [FM] is kept constant while the ratio [T]/[FM] varies.[36] The absorption is plotted as a function of the molar fraction of one of the two components. A maximum value in the graph indicates the presence of a complex with a composition of $L_mFM_n$ where the molar ratio, $x$, at the maximum represents the complexation stoichiometry. A maximum appearing at $x = 0.14$ indicates that a 1:6 complex is the predominant structure at equilibrium conditions. This result showed good agreement with calculations from the computational approach (Figure 3) that the ratio of T: FM was 1:6.

## 3.5 | Preparation of the MIP and NIP

The following ratios were used for this synthesis: the template: monomer:crosslinker ratio for MIP1 and MIP3 was 1:6:20, while for MIP2 and MIP 4 it was 1:4:20. MIP1 and MIP3 used the ratio from the computational approach and Jobs results, while MIP 2 and MIP 4 used the ratio from the study of Pratama et al.,[37] which demonstrated that the use of template–monomer (1:4) provides an excellent specific affinity and high recovery of template compound compared with NIP sorbents. The bulk method was used for the synthesis of MIPs and NIPs. Bulk polymerization has the advantages of being operationally simple and inexpensive.[38] Two different compositions were used to see whether the computational approach and the Jobs results were in good agreement with wet lab experiments on blood sample extraction. Two kind of crosslinker (EDGMA and TRIM) were used to see the agreement with crosslinker selection on computational approach result.

## 3.6 | Adsorption capacity evaluation

The adsorption capacity of MIP and NIP can be determined using the adsorption isotherm model. Isotherms can be matched using different models with different assumptions. The results obtained (Table 5) show that the data of some MIPs fitted well with the Langmuir isotherm, which indicated the homogenous nature of binding sites, while the others fitted with Freundlich, which indicated the heterogeneous nature of binding sites.

The parameters of the two isotherm models are listed in Table 5. The correlation coefficient of MIP 1 is 0.9334 for the Langmuir isotherm model which is used to describe the monolayer adsorption by homogeneous binding sites. From the correlation coefficient ($R$) value, it can be obtained that MIP 1 is has good fitting to the Langmuir model while the others (MIP 2, MIP 3 and MIP 4) more suitable with Freundlich model. It shows that MIP 2, MIP 3, and MIP 4 have more heterogeneous binding site than MIP1. The differences in adsorption intensity ($a$) of all polymers indicates the great differences in the affinity of the binding sites.[39] MIP 3 has higher adsorption intensity than others. The heterogeneity index ($m$) values of NIP 2, NIP 3, and NIP 4 are close to 0, which means that there are more heterogeneous binding sites on the surface of the polymer.[40]

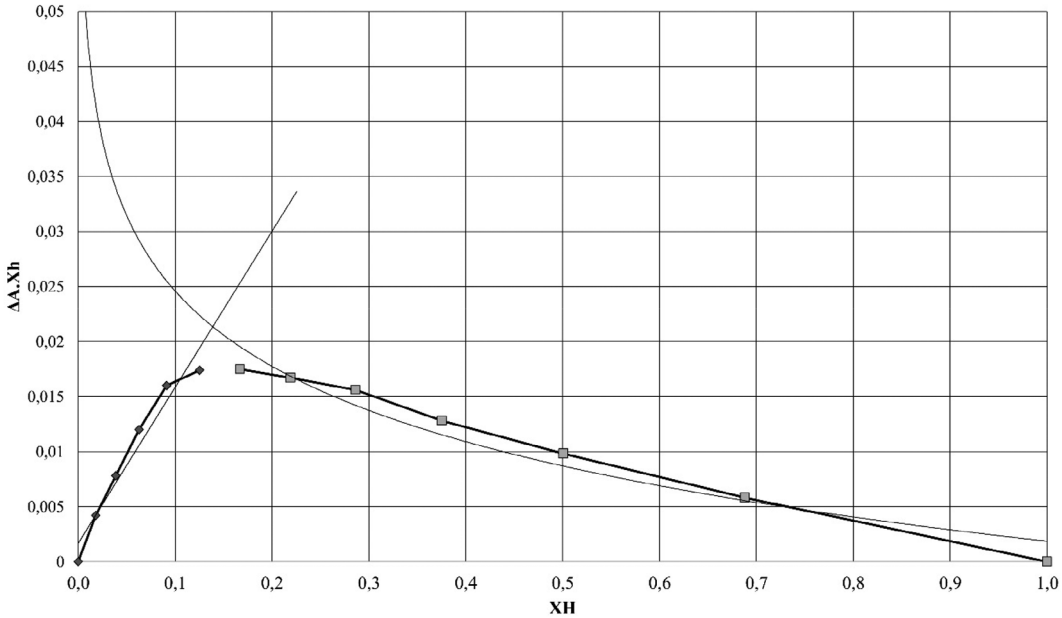


**FIGURE 3** Jobs plot of SLX-HEMA complex

**TABLE 5** Fitting data to isotherm model

| | Langmuir | | | Freundlich | | |
|---|---|---|---|---|---|---|
| Polymer | *R* | $K_L$ (L.mg) | $Q_m$ (mg.g$^{-1}$) | *R* | *m* | *a* (mg.g$^{-1}$) |
| MIP1 | 0.9334 | 0.3131 | 0.4278 | 0.7778 | 0.0625 | 0.1230 |
| NIP1 | 0.9726 | 1.4413 | 0.1023 | 0.5312 | 0.0210 | 0.0308 |
| MIP2 | 0.8664 | 0.854 | 0.3927 | 0.9381 | 0.7108 | 0.0508 |
| NIP2 | 0.7342 | 0.5823 | 0.1016 | 0.1532 | 0.1410 | 0.0594 |
| MIP3 | 0.9737 | 0.1983 | 1.7235 | 0.9755 | 0.7515 | 0.2847 |
| NIP3 | 0.9990 | 0.0551 | 1.4257 | 0.9997 | 0.8447 | 0.0789 |
| MIP4 | 0.9882 | 0.1193 | 1.7784 | 1 | 0.7704 | 0.1973 |
| NIP4 | 0.9653 | 0.1308 | 0.6533 | 0.9835 | 0.7094 | 0.0823 |

Abbreviations: MIP, molecular imprinted polymer; NIP, non-imprinted polymer.

## 3.7 | Optimization of the MISPE condition

Optimization was carried out by employing a solution of 2 mg L$^{-1}$ of SLX in isopropanol or deionized water as the sample. SPE parameters investigated include conditioning, loading, washing, and elution solvents. In the first step, methanol was selected as the conditioning solvent, and a series of experiments using all MIP and NIP cartridges were carried out. The organic solvents strongly influence the configuration of the polymer network, consequently changing the pore volume and surface area.[41]

Loading of solvents was done by using two solvents, which were isopropanol and water. To have better interaction between SLX and MIP, the effect of the polarity of the loading solvent must be considered.[42] Isopropanol was chosen because it has lower polarity and it was predicted that it will not interfere with the interaction of SLX with MIP, while deionized water was used to resemble with real sample.

The next step in MISPE optimization is the washing step. Washing is a crucial step in developing an MISPE procedure because the general procedure for reducing problems of non-specific adsorption is the selection of a proper washing solvent prior to elution.[43] As can be seen in Figure 4A, acetonitrile is excellent solvent for washing. The recovery was 0.57% ± 0.12% for MIP3 and 16.09% ± 1.31% for NIP3. The strong imprint–analyte interaction must be destroyed to reach a high extraction recovery. The expected protonation of SLX can promote the disruption of the hydrogen bonds between SLX and MIP.[44] For this task, an acid pH is required, so a mixture of methanol–acetic acid (99:1) was used

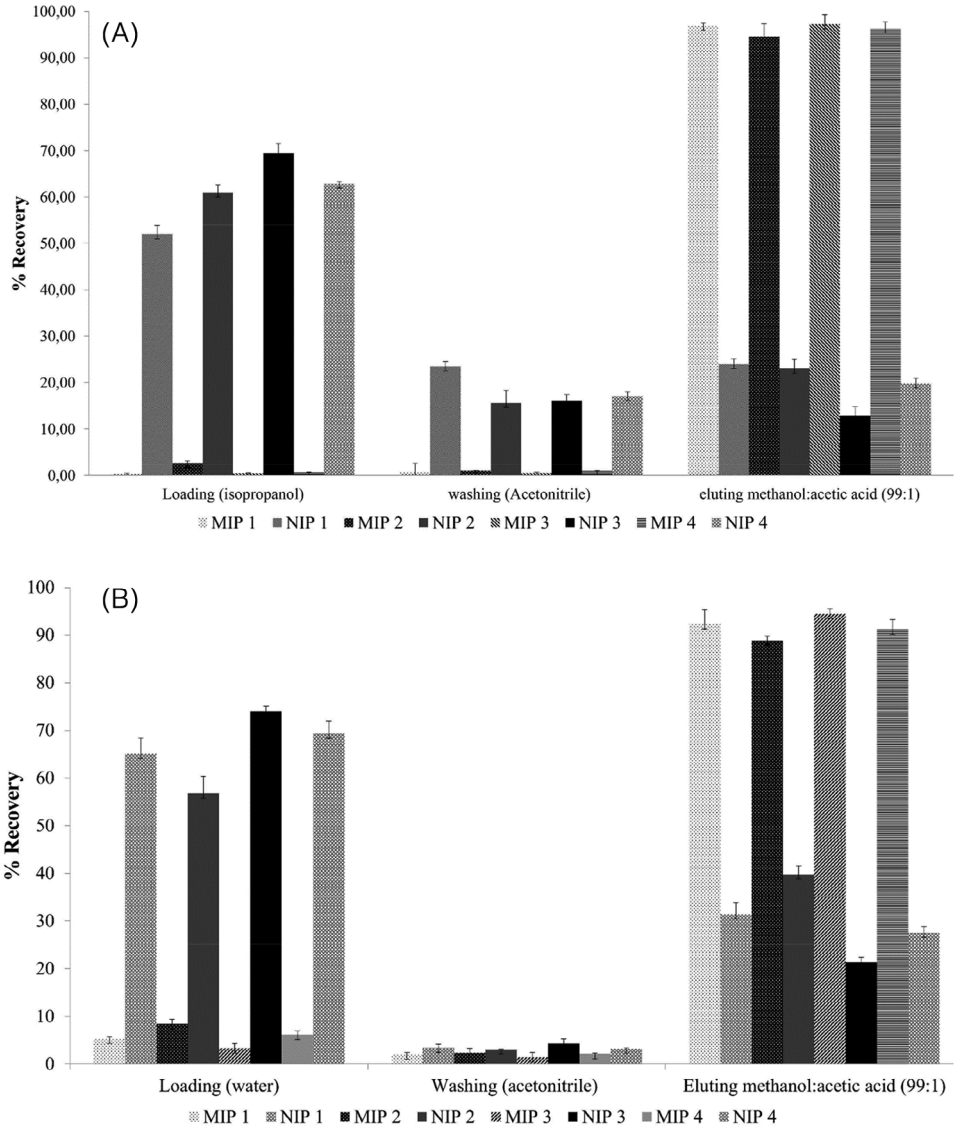


**FIGURE 4** (A) molecularly imprinted solid-phase extraction (MISPE) optimization with loading of isopropanol. (B) MISPE optimization with loading of deionized water

for its elution from the SPE cartridge. The elution was done with 4 × 1 ml of elution solvent. The final recovery showed values of 96.23% ± 0.82% and 12.05% ± 1.56% for MIP 3 and NIP 3, respectively, for a sample loaded in isopropanol. This means the imprinting factor for MIP 3 was 7.99, which shows the efficiency of imprinting. The specific interaction between analyte and imprint-site was more dominant in MIP3 than the nonspecific interaction showed by NIP3. Tables 5 and 6 show the recovery of SLX with isopropanol and deionized water as loading solvents. In order to mimic the real conditions of SLX in serum, the other loading condition was provided by water. As seen in Figure 4B, the final recoveries with this solvent were lower than isopropanol for all MIPs, especially for MIP 3 with recovery percentage of 92.17% ± 2.66%.

MIP 3 was used for further testing of MIP performance in serum as this MIP has the best recovery percentage. MIP 3 was made with a 1:6 ratio of T:FM and TRIM as crosslinker. It showed the greatest recovery, which means that there is agreement between the results of the computation simulation and constant association experiments in comparison with the 1:4 ratio (common ratio) and EGDMA as crosslinker. The ratio of T-FM showed the

**TABLE 6** Application MISPE to serum spiked with SLX loading with deionized water

| Polymer | % Recovery | IF |
|---|---|---|
| MIP 1 | 90.44 ± 1.82 | 2.30 |
| NIP 1 | 39.31 ± 1.15 | |
| MIP 2 | 87.41 ± 1,15 | 2.11 |
| NIP 2 | 41.52 ± 6.77 | |
| MIP 3 | 92.17 ± 2.66 | 3.44 |
| NIP 3 | 26.78 ± 2.39 | |
| MIP 4 | 88.57 ± 4.50 | 2.35 |
| NIP 4 | 37.61 ± 3.60 | |

Abbreviations: MIP, molecular imprinted polymer; MISPE, molecularly imprinted solid-phase extraction; NIP, non-imprinted polymer.

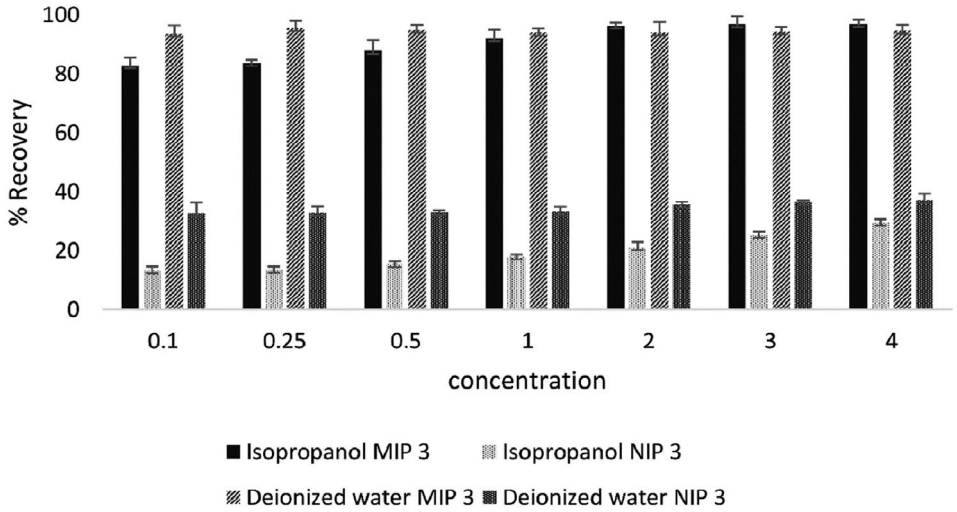


**FIGURE 5** Effect of different SLX concentrations on percent recovery, loading with isopropanol and deionized water

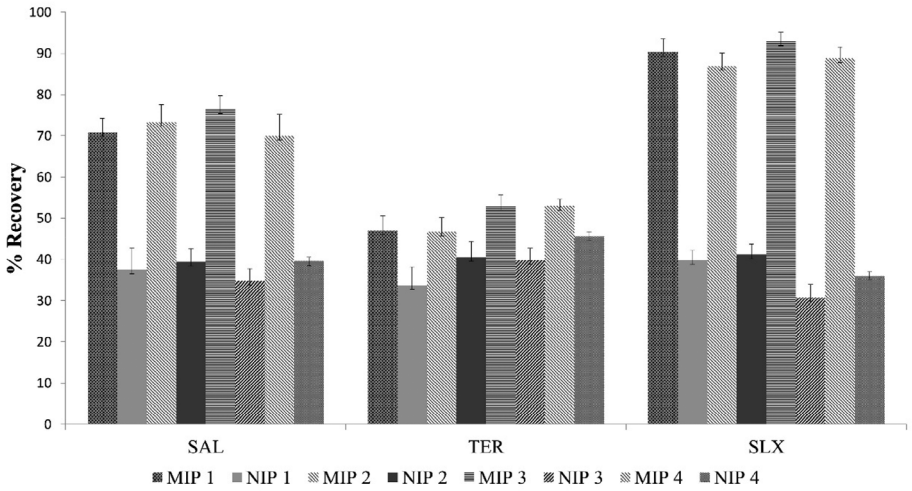


**FIGURE 6** Selectivity test molecularly imprinted solid-phase extraction (MISPE) compared to another analogous structures (loading with deionized water)

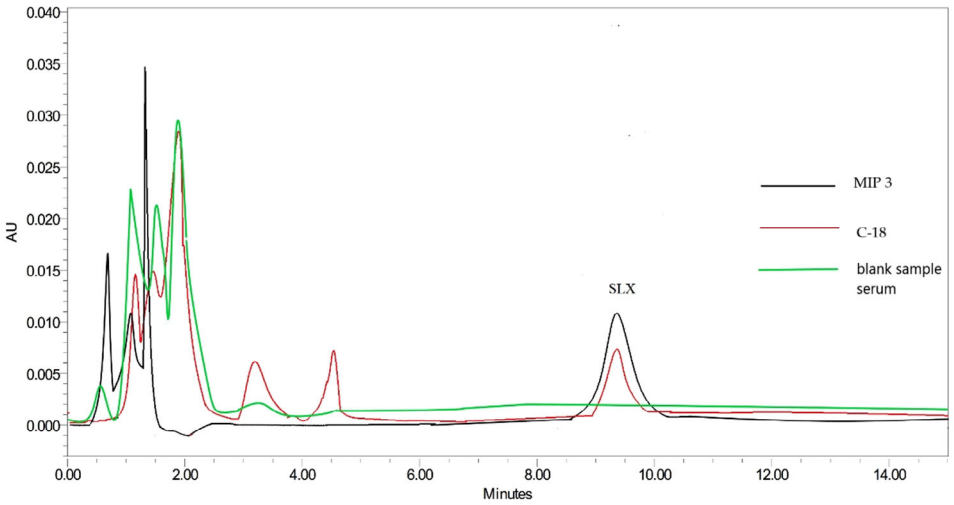


**FIGURE 7** Chromatogram of C-18 and molecular imprinted polymer (MIP) 3 on extraction of SLX from spiked serum

**TABLE 7** Comparison of repeatability, recovery, and LOQ values with other research studies

| | Other research[6,7] | Our results |
|---|---|---|
| Repeatability (%RSD) | 4.5;13.7 | 4.21 |
| Recovery (%) | 103.6; 98.3 | 92.17 |
| LOQ (ng $ml^{-1}$) | 0.5; 0.0025 | 4.62 |

Abbreviation: LOQ, limit of quantitation.

significance of its role in polymer performance, exactly according to the theory.[45]

## 3.8 | Effect of concentration loading to extraction of SLX

The concentration of the loading concentration must be considered to optimize of MISPE. Ideally, recovery of extraction should not depend on the concentration of the sample. In other words, there ought to be no prominent difference in recovery at all ranges of concentrations that are analyzed.[46] However, on this research, on loading using isopropanol, as seen in Figure 6, the template's selectivity and affinity were preferable at higher concentrations. For MIP 3, the recovery of 0.1 mg $L^{-1}$, as the lowest concentration, was 82.84% ± 2.62%, while at 4 mg $L^{-1}$, as the highest concentration, it was 96.96% ± 1.35%. Although the lower recovery was achieved on 0.1 mg $L^{-1}$, it still fulfilled the FDA requirement of recovery of a drug from a biological matrix (80%).[47] The phenomenon arise on loading using propanol that depends on concentration because at greater concentrations, the capability of SLX to produce SLX-SLX complexes, both on the surface of the polymer and in the solution, brought an increased selectivity of SLX.[48] This phenomenon wasn't found when water was used as the loading solvent. As seen in Figure 5, the recovery of extractions was similar for all test concentrations in water. The hydrogen bonding capacity of the solvent in the loading solution corresponds with the recognition properties.[49] Water has a higher hydrogen bonding capacity than isopropanol, thereby preventing the formation of SLX-SLX complexes due to competition on the site of hydrogen bonding of molecules.[50] On the other hand, this nature of water as a solvent with strong hydrogen bonding capability can interfere with interaction between SLX with active site moieties on the polymer that can reduce the adsorption capacity. The higher recovery of SLX in water than isopropanol on lower concentrations is most likely due to a swelling effect of polymer more suitable in aqueous conditions.[51,52] This result is similar to the study by Xia et al.[53] that found analyte recoveries after using water solvent as the loading solvents were higher than those obtained when methanol and acetonitrile were used. According to this result, water is more preferable to be used as a loading solvent as the recovery result did not depend on the concentration and can extract SLX in lower to highest concentration with the constant recovery result compared to isopropanol.

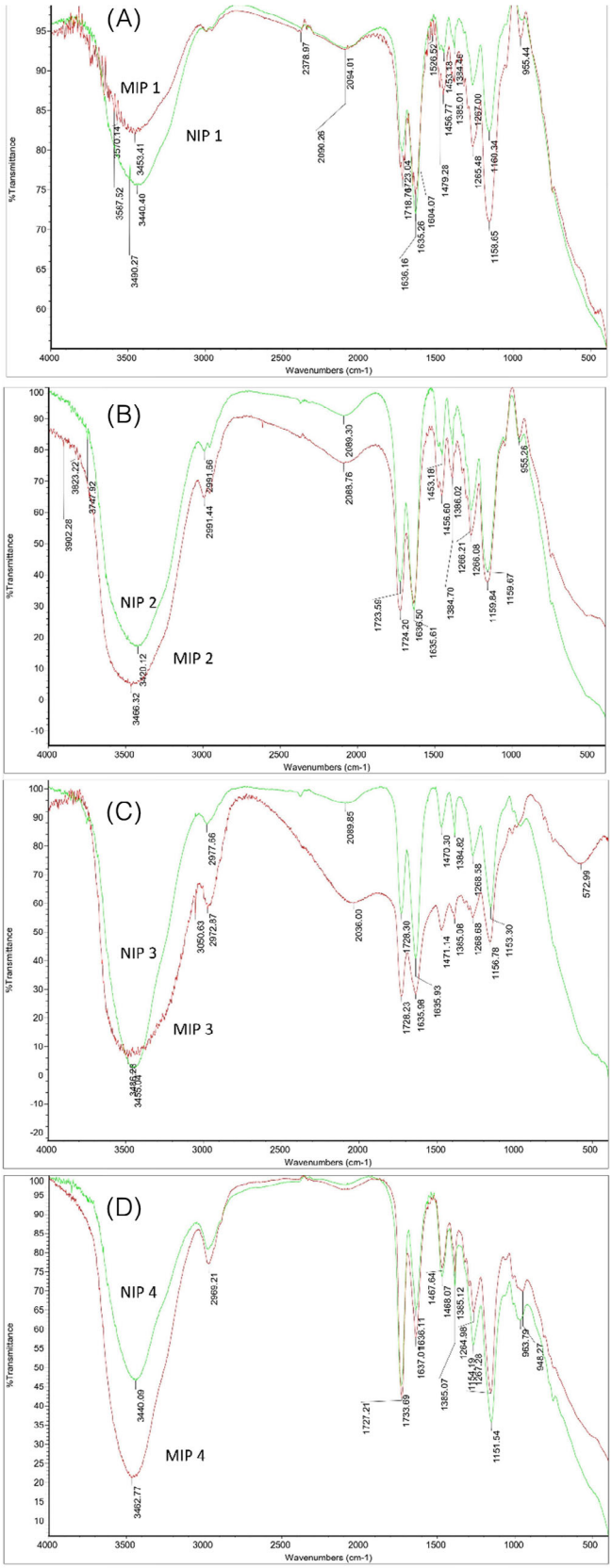


**FIGURE 8** Fourier transform infra-red (FTIR) spectra of molecular imprinted polymer (MIP) 1 and non-imprinted polymer (NIP) 1 (A), MIP 2 and NIP 2 (B), MIP 3 and NIP 3 (C), MIP 4 and NIP 4 (D)

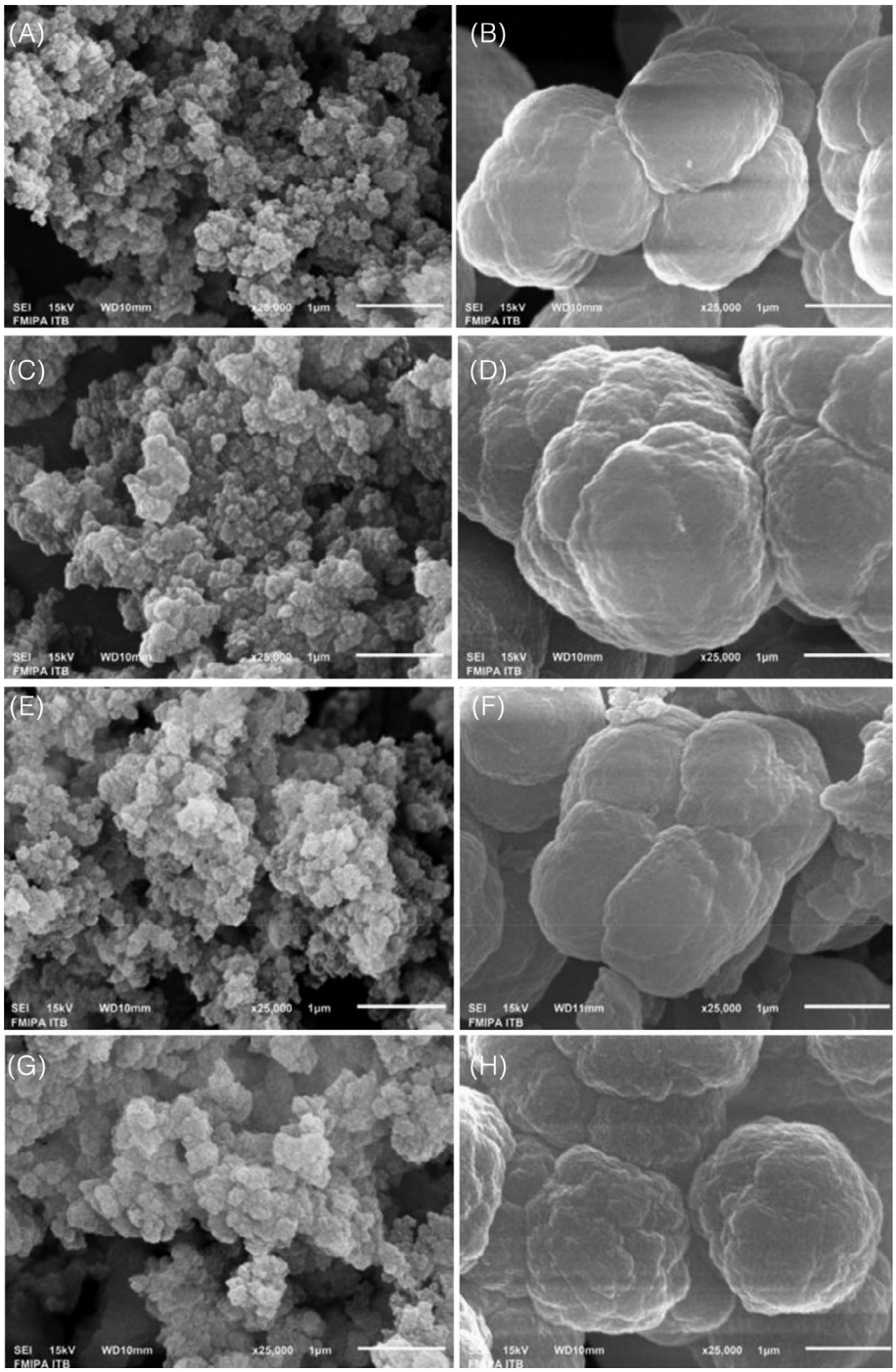


**FIGURE 9** Scanning electron microscope (SEM) of molecular imprinted polymer (MIP) 1 (A), non-imprinted polymer (NIP) 1 (B), MIP 2 (C), NIP 2 (D), MIP 3 (E), NIP 3 (F), MIP 4 (G), and NIP 4 (H)

### 3.9 | Application of polymer to extract SLX from spiked serum, selectivity testing, and comparison with the C-18 cartridge

Using the optimized condition for MISPE, the higher recoveries of spiked serum containing 2 mg $L^{-1}$ of SLX in water were obtained by MIP 3. The recoveries results showed that the mol ratio of 1:6 T-FM and TRIM as the crosslinker was the best combination of MIP formulation to extract SLX from a biological sample (serum). As shown in Table 6, the recovery of all MIPs was higher than 80%. For MIP3, a high recovery was achieved (92.17% ± 2.66%). The higher IF of MIP3 indicated that the imprinting efficiency of MIP3 was better than the others and showed best affinity and selectivity of the polymer. According to theory,[54] the main driving force for a molecule to diffuse into and migrate through a polymer is its affinity to the binding pockets. The diffusion is related to dipole–dipole interactions and Van der Waals forces, the friction forces within the crosslinked polymer will determine the rate at which the molecules permeate.[55] The recovery of SLX from spiked serum by MIPs fulfills EMA and FDA's standards for recovery of a drug from a biological matrix, which must be higher than 80%.[56]

To evaluate the recognition properties of synthesized MIPs, structural analogues of SLX such as SAL and TER were employed to carry out the competitive rebinding studies using MISPE. The selectivity of the MISPE sorbent was determined by comparing the IF values

among SLX, SAL, and TER.[57] The selectivity factor can be attributed to the differences in their molecular shapes and size compared to SLX. On MIP, SLX and competitors interacted with the binding site (cavity) on adsorbent with specific interaction, while on NIP, they interacted nonspecific. Sites arising from any form of monomer-template complex in the pre-polymerization mixture, are expected to have a higher affinity for template and similar structures.[54] The MIP can differentiate the SLX with SAL and TER due to the precise arrangement of the functional group and shape selectivity of the synthesized MIP. Nonspecific binding is likely due to interaction with a randomly dispersed functional group in the polymer. The majority of the binding was credited to nonspecific hydrophobic binding, interaction with reactive acidic moieties on the surface of the polymer.[54] As is evident from this study, there is a substantial degree of reactivity of the MIP toward SAL and TER. This effect is not observed in the NIP (Figure 6), indicating that the binding is specific and not due to hydrophobic binding. All three of the molecules possess similar functionalities, it can be seen that both of molecules will be capable of undergoing similar functional interactions with HEMA as SLX. Since the molecules are different, it is likely that spatial complementary plays a role in the selectivity observed. The difference in the spatial arrangement of molecules and functionalities are responsible for the differences in selectivity between SLX and the analogues.

To further validate the selectivity of MISPE, C18 cartridges were purchased and tested for the adsorption of SLX in the spiked serum, and the result is exhibited in Figure 7. Extraction of SLX from spiked serum with C-18 cartridges showed lower percent recovery (79.11% ± 2.96%) than MIPs, and this can be due to the interference of the matrix. The results showed that the conventional C-18 sorbent is less selective than MIPs.

The HPLC method for SLX analysis was validated according to the FDA and EMA guideline for bioanalysis.[56] Using these conditions, the limit of detection (LOD) and limit of quantitation (LOQ) for SLX were 1.38 and 4.62 ng $ml^{-1}$ respectively, linear coefficient correlation was ($R$) = 0.9995 with, % RSD = 4.21 Comparison of the method result is given in Table 7. From the table, we could see that the method is comparable with another research on SLX analysis in blood plasma with more sensitive method namely LC/MS/MS assays.[6,7] This results showed that our study have good repeatability and recovery results are not too far in comparison with the latter.[6,7]

### 3.10 | FTIR, SEM, and BET measurement of MIP

The FTIR analysis of sorbents, depicted in Figure 8, shows that MIPs have a spectrum that is almost identical to the NIPs spectrum, indicating that SLX has been extracted from the MIP matrix.[58] The absence of twin peaks in the wave number 900–1000 $cm^{-1}$ indicates the absence of a vinyl group which means the polymerization process is complete.[59] The morphology of MIPs was characterized using SEM. Figure 9 shows that the sorbents have smaller particle sizes with higher porosity compared to sorbent NIPs. The higher porosity level of MIP compared to NIP shows that the MIP has formed a cavity or recognition side to the target molecule,[60] with a high porosity profile allowing a greater adsorption area so that it can provide good adsorption ability at SLX. The BET surface area were detected by nitrogen adsorption measurement. As seen in Table 8, The BET surface area of MIP 3 was highest among others. The MIP 3 showed a specific surface area of 221.757 $m^2$ $g^{-1}$, which were three times larger than that of NIP 3 (61.381 $m^2$ $g^{-1}$), This was attributed to the cavities created by the imprinting process.[61] The result of SEM and BET characterization indicated the enhancement in surface of the MIPs due to the imprinting of the template molecule.[62]

**TABLE 8** Multipoint Brunauer–Emmett–Teller result for MIPs and NIPs

| Sorbent | Surface area ($m^2$ $g^{-1}$) |
|---|---|
| MIP 1 | 42.297 |
| NIP 1 | 18.367 |
| MIP 2 | 40.674 |
| NIP 2 | 6.033 |
| MIP 3 | 221.757 |
| NIP 3 | 61.381 |
| MIP 4 | 141.370 |
| NIP 4 | 37.131 |

Abbreviations: MIP, molecular imprinted polymer; NIP, non-imprinted polymer.

## 4 | CONCLUSIONS

In conclusion, the results presented here demonstrate the usefulness of computational methods for rapid screening of FMs and crosslinkers for a specified template molecule in an experiment-free way. According to the theoretical calculations, HEMA and TRIM were selected as the FM and crosslinker, respectively. The new sorbent revealed good selectivity toward the SLX molecule over other structurally related compounds. The high extraction recovery, high selectivity, and the high physical and chemical robustness of the synthesized MIP enabled its applicability as a promising sorbent for MISPE applications.

### ACKNOWLEDGMENTS

Financial support by Directorate General of Higher Education, Ministry of Education and Culture Indonesia is gratefully acknowledged.

### DATA AVAILABILITY STATEMENT

The data that support the findings of this study are available from the corresponding author upon reasonable request.

### ORCID

*Shendi Suryana* https://orcid.org/0000-0002-0849-0003
*Aliya Nur Hasanah* https://orcid.org/0000-0002-4085-7872

## REFERENCES


1. Cazzola M, Matera MG. Review: safety of long-acting β2 -agonists in the treatment of asthma. *Ther Adv Respir Dis*. 2007;1(1):35-46. https://doi.org/10.1177/1753465807081747
2. Chengalva P, Kuchana M. Development and validation of ultra performance liquid chromatographic method for the analysis of pulmonary drug product containing formoterol fumarate and fluticasone propionate. *Int Res J Pharm*. 2018;9(9):152-157. https://doi.org/10.7897/2230-8407.099204
3. Lommatzsch M, Lindner Y, Edner A, Bratke K, Kuepper M, Virchow JC. Adverse effects of salmeterol in asthma: a neuronal perspective. *Thorax*. 2009;64(9):763-769. https://doi.org/10.1136/thx.2008.110916
4. Deventer K, Pozo OJ, Delbeke FT, Van Eenoo P. Quantitative detection of inhaled salmeterol in human urine and relevance to doping control analysis. *Ther Drug Monit*. 2011;33(5):627-631.
5. Jacobson GA, Fawcett JP. Beta2-agonist doping control and optical isomer challenges. *Sport Med*. 2016;46(12):1787-1795. https://doi.org/10.1007/s40279-016-0547-4
6. Silvestro L, Savu SR, Savu SN, Tudoroniu A, Tarcomnicu I. Development of a sensitive method for simultaneous determination of fluticasone propionate and salmeterol in plasma samples by liquid chromatography-tandem mass spectrometry. *Biomed Chromatogr*. 2012;26(5):627-635. https://doi.org/10.1002/bmc.1708
7. Čápka V, Carter SJ. Minimizing matrix effects in the development of a method for the determination of salmeterol in human plasma by LC/-MS/MS at low pg/mL concentration levels. *J Chromatogr B Anal Technol Biomed Life Sci*. 2007;856(1–2):285-293. https://doi.org/10.1016/j.jchromb.2007.06.010
8. Marchi I, Rudaz S, Veuthey JL. Sample preparation development and matrix effects evaluation for multianalyte determination in urine. *J Pharm Biomed Anal*. 2009;49(2):459-467. https://doi.org/10.1016/j.jpba.2008.11.040
9. Lendoiro E, De Castro A. Molecularly imprinted polymer for selective determination of Δ9-tetrahydrocannabinol and 11-nor-Δ9-tetrahydrocannabinol carboxylic acid using LC-MS/MS in urine and oral fluid. *Anal Bioanal Chem*. 2014;406:3589-3597. https://doi.org/10.1007/s00216-013-7599-1
10. Tang T, Wei F, Wang X, et al. Determination of semicarbazide in fish by molecularly imprinted stir bar sorptive extraction coupled with high performance liquid chromatography. *J Chromatogr B Anal Technol Biomed Life Sci*. 2018;1076:8-14. https://doi.org/10.1016/j.jchromb.2018.01.003
11. Ncube S, Madikizela LM, Nindi MM, Chimuka L. *Solid Phase Extraction Technique as a General Field of Application of Molecularly Imprinted Polymer Materials*. 1st ed. Elsevier B.V.; 2019.
12. Möller K. *Molecularly Imprinted Solid-Phase Extraction and Liquid Chromatography/Mass Spectrometry for Biological Samples*; Stockholm University; 2006. doi:https://doi.org/10.1002/yea
13. Díaz-Álvarez M, Martín-Esteban A. Sample preparation via molecularly imprinted polymers (MIPs) in LC-MS bioanalysis. *Sample Prep LC-MS Bioanal*. 1981;2019:139-151. https://doi.org/10.1002/9781119274315.ch11
14. Pan J, Chen W, Ma Y, Pan G. Molecularly imprinted polymers as receptor mimics for selective cell recognition. *Chem Soc Rev*. 2018;47(15):5574-5587. https://doi.org/10.1039/c7cs00854f
15. Ao J, Gu J, Yuan T, Li D, Ma Y, Shen Z. Applying molecular modelling and experimental studies to develop molecularly imprinted polymer for domoic acid enrichment from both seawater and shellfish. *Chemosphere*. 2018;199(800):98-106. https://doi.org/10.1016/j.chemosphere.2018.02.005
16. Tadi KK, Motghare RV. Rational synthesis of pindolol imprinted polymer by non-covalent protocol based on computational approach. *J Mol Model*. 2013;19(8):3385-3396. https://doi.org/10.1007/s00894-013-1856-2
17. Marć M, Kupka T, Wieczorek PP, Namieśnik J. Computational modeling of molecularly imprinted polymers as a green approach to the development of novel analytical sorbents. *Trends Anal Chem*. 2018;98:64-78. https://doi.org/10.1016/j.trac.2017.10.020
18. Olsson GD, Karlsson BCG, Shoravi S, Wiklander JG, Nicholls IA. Mechanisms underlying molecularly imprinted polymer molecular memory and the role of crosslinker: resolving debate on the nature of template recognition in phenylalanine anilide imprinted polymers. *J Mol Recognit*. 2012;25(2):69-73. https://doi.org/10.1002/jmr.2147
19. Zeng H, Wang Y, Liu X, Kong J, Nie C. Preparation of molecular imprinted polymers using bi-functional monomer and bi-crosslinker for solid-phase extraction of rutin. *Talanta*. 2012;93:172-181. https://doi.org/10.1016/j.talanta.2012.02.008
20. Li H, Zhang W, Wu Z, et al. Theoretical design, preparation, and evaluation of ginkgolide B molecularly imprinted polymers. *J Sep Sci*. 2020;43(2):514-523. https://doi.org/10.1002/jssc.201900675
21. Zhang B, Fan X, Zhao D. Computer-aided design of molecularly imprinted polymers for simultaneous detection of clenbuterol and its metabolites. *Polymers (Basel)*. 2018;11(1):1-21. https://doi.org/10.3390/polym11010017
22. Ganjavi F, Ansari M, Kazemipour M, Zeidabadinejad L. Computational design, synthesis and utilization of a magnetic molecularly imprinted polymer on graphene oxide nanosheets for highly selective extraction and determination of buprenorphine in biological fluids and tablets. *Anal Methods*. 2018;10(43):5214-5226. https://doi.org/10.1039/c8ay01757c
23. Dong C, Li X, Guo Z, Qi J. Development of a model for the rational design of molecular imprinted polymer: computational approach for combined molecular dynamics/quantum mechanics calculations. *Anal Chim Acta*. 2009;647(1):117-124. https://doi.org/10.1016/j.aca.2009.05.040
24. Viveiros R, Karim K, Piletsky SA, Heggie W, Casimiro T. Development of a molecularly imprinted polymer for a pharmaceutical impurity in supercritical CO2: rational design using computational approach. *J Clean Prod*. 2017;168:1025-1031. https://doi.org/10.1016/j.jclepro.2017.09.026
25. Suryana S, Mutakin RY, Hasanah AN. An update on molecularly imprinted polymer design through a computational approach to produce molecular recognition material with enhanced analytical performance. *Molecules*. 2021;26(7):1-20. https://doi.org/10.3390/molecules26071891
26. Amin S, Damayanti S, Ibrahim S. Interaction binding study of dimethylamylamine with functional monomers to design a molecular imprinted polymer for doping analysis. *J Appl Pharm Sci*. 2018;8(10):25-31. https://doi.org/10.7324/JAPS.2018.81004
27. Garg M, Naidu R, Birhade A, et al. Bioequivalence of two formulations of salmeterol xinafoate/fluticasone propionate HFA pMDI in healthy volunteers. *J Bioequiv Availab*. 2017;09(06):536-546. https://doi.org/10.4172/jbb.1000359
28. Liu J, Zhao W, Wang G, Tang S, Jin R. Simulation of a phenobarbital molecularly imprinted polymerization self-assembly system and its adsorption property. *Anal Methods*. 2020;12(6):813-821. https://doi.org/10.1039/c9ay02539a
29. Yang DP, Zhang QL, Song XY, Cheng SB. Modulating mechanism of N[sbnd]H-based excited-state intramolecular proton transfer by electron-withdrawing substituent at aromatic para-position. *Chem Phys Lett*. 2019;730(April):76-83. https://doi.org/10.1016/j.cplett.2019.05.039
30. Krishnan H, Islam KMS, Hamzah Z, Ahmad MN. Rational computational design for the development of andrographolide molecularly imprinted polymer. *AIP Conference Proceedings*. Vol 1891. AIP Publishing; 2017. https://doi.org/10.1063/1.5005416
31. Estarellas C, Escudero D, Frontera A, Quiñonero D, Deyà PM. Theoretical ab initio study of the interplay between hydrogen bonding, cation-π and π-π interactions. *Theor Chem Acc*. 2009;122(5–6):325-332. https://doi.org/10.1007/s00214-009-0517-0
32. Yan H, Ho RK. Characteristic and synthetic approach of molecularly imprinted polymer. *Int J Mol Sci*. 2006;7:155-178. https://doi.org/10.3390/i7050155
33. Muhammad T, Nur Z, Piletska EV, Piletsky SA. Rational design of molecularly imprinted polymer: the choice of cross-linker. *Analyst*. 2012;137:2623-2628. https://doi.org/10.1039/c2an35228a

34. Shoravi S, Olsson GD, Karlsson BCG, Nicholls IA. On the influence of crosslinker on template complexation in molecularly imprinted polymers: a computational study of prepolymerization mixture events with correlations to template-polymer recognition behavior and NMR spectroscopic studies. *Int J Mol Sci*. 2014;15:10622-10634. https://doi.org/10.3390/ijms150610622
35. Cabot R, Hunter CA, Varley LM. Hydrogen bonding properties of non-polar solvents. *Org Biomol Chem*. 2010;8(6):1455-1462. https://doi.org/10.1039/b921003b
36. Renny JS, Tomasevich LL, Tallmadge EH, Collum DB. Method of continuous variations: applications of job plots to the study of molecular associations in organometallic chemistry. *Angew Chem Int Ed*. 2013;52(46):11998-12013. https://doi.org/10.1002/anie.201304157
37. Pratama KF, Manik MER, Rahayu D, Hasanah AN. Effect of the molecularly imprinted polymer component ratio on analytical performance. *Chem Pharm Bull*. 2020;68(11):1013-1024. https://doi.org/10.1248/cpb.c20-00551
38. He JX, Pan HY, Xu L, Tang RY. Application of molecularly imprinted polymers for the separation and detection of aflatoxin. *J Chem Res*. 2020;45:400-410. https://doi.org/10.1177/1747519820980373
39. Ayawei N, Ebelegi AN, Wankasi D. Modelling and interpretation of adsorption isotherms. *J Chem*. 2017;2017:1-11. https://doi.org/10.1155/2017/3039817
40. Kumar KV, Gadipelli S, Wood B, et al. Characterization of the adsorption site energies and heterogeneous surfaces of porous materials. *J Mater Chem A*. 2019;7(17):10104-10137. https://doi.org/10.1039/c9ta00287a
41. Chrzanowska AM, Diaz-Alvares M, Wieczorek PP, Poliwoda A, Martin-Esteban A. The application of the supported liquid membrane and molecularly imprinted polymers as solid acceptor phase for selective extraction of biochanin A from urine. *J Chromatogr A*. 2019;1599:9-16. https://doi.org/10.1016/j.chroma.2019.04.005
42. Ahmadi F, Ahmadi J, Rahimi-Nasrabadi M. Computational approaches to design a molecular imprinted polymer for high selective extraction of 3,4-methylenedioxymethamphetamine from plasma. *J Chromatogr A*. 2011;1218(43):7739-7747. https://doi.org/10.1016/j.chroma.2011.08.020
43. Ahmadi F, Sadeghi T, Ataie Z, Rahimi-Nasrabadi M, Eslami N. Computational design of a selective molecular imprinted polymer for extraction of pseudoephedrine from plasma and determination by HPLC. *Anal Chem Lett*. 2017;7(3):295-310. https://doi.org/10.1080/22297928.2017.1353920
44. Niskanen J, Sahle CJ, Juurinen I, et al. Protonation dynamics and hydrogen bonding in aqueous sulfuric acid. *J Phys Chem B*. 2015;119(35):11732-11739. https://doi.org/10.1021/acs.jpcb.5b04371
45. Xie L, Xiao N, Li L, Xie X, Li Y. Theoretical insight into the interaction between chloramphenicol and functional monomer (methacrylic acid) in molecularly imprinted polymers. *Int J Mol Sci*. 2020;21(11):1-14. https://doi.org/10.3390/ijms21114139
46. Maranata GJ, Surya NO, Hasanah AN. Optimising factors affecting solid phase extraction performances of molecular imprinted polymer as recent sample preparation technique. *Heliyon*. 2021;7(1):e05934. https://doi.org/10.1016/j.heliyon.2021.e05934
47. FDA-U.S. Department of Health and Human Services. Analytical Procedures and Methods Validation for Drugs and Biologics. Guidance Document. July; 2015:1-15. http://www.ich.org/fileadmin/Public_Web_Site/ICH_Products/Guidelines/Quality/Q2_R1/Step4/Q2_R1__Guideline.pdf
48. Koohpaei AR, Shahtaheri SJ, Ganjali MR, Forushani AR, Golbabaei F. Molecular imprinted solid phase extraction for determination of atrazine in environmental samples. *Iran J Environ Heal Sci Eng*. 2008;5(4):283-296.
49. Zhang Y, Qu X, Wang FF, et al. Effect of the solvent on improving the recognition properties of surface molecularly imprinted polymers for precise separation of erythromycin. *RSC Adv*. 2015;5(102):83619-83627. https://doi.org/10.1039/c5ra09497f
50. Alavi S, Takeya S, Ohmura R, Woo TK, Ripmeester JA. Hydrogen-bonding alcohol-water interactions in binary ethanol, 1-propanol, and 2-propanol+methane structure II clathrate hydrates. *J Chem Phys*. 2010;133(7):1-9. https://doi.org/10.1063/1.3469776
51. Wang XH, Xie LF, Dong Q, Liu HL, Huang YP, Liu ZS. Synthesis of monodisperse molecularly imprinted microspheres with multi-recognition ability via precipitation polymerization for the selective extraction of cyromazine, melamine, triamterene and trimethoprim. *J Chromatogr B Anal Technol Biomed Life Sci*. 2015;1007:127-131. https://doi.org/10.1016/j.jchromb.2015.11.009
52. Pardeshi S, Dhodapkar R, Kumar A. Influence of porogens on the specific recognition of molecularly imprinted poly(acrylamide-co-ethylene glycol dimethacrylate). *Compos Interfaces*. 2015;21:37-41. https://doi.org/10.1080/15685543.2013.830515
53. Xia WQ, Cui PL, Wang GN, Liu J, Wang JP. Application of dual-template molecularly imprinted polymer-based solid phase extraction for determination of phenothiazines and benzodiazepines in swine feed. *Anal Methods*. 2018;10(25):3001-3010. https://doi.org/10.1039/c8ay00873f
54. Ansell RJ. Characterization of the binding properties of molecularly imprinted polymers. *Adv Biochem Eng Biotechnol*. 2015;150:51-93. https://doi.org/10.1007/10_2015_316
55. Farrington K, Magner E, Regan F. Predicting the performance of molecularly imprinted polymers: selective extraction of caffeine by molecularly imprinted solid phase extraction. *Anal Chim Acta*. 2006;566(1):60-68. https://doi.org/10.1016/j.aca.2006.02.057
56. Smith G. European medicines agency guideline on bioanalytical method validation: what more is there to say? *Bioanalysis*. 2012;4(8):865-868. https://doi.org/10.4155/bio.12.44
57. Cazzola M, Testi R, Matera MG. Clinical pharmacokinetics of salmeterol. *Clin Pharmacokinet*. 2002;41(1):19-30.
58. Hasanah AN, Rahayu D, Pratiwi R, et al. Extraction of atenolol from spiked blood serum using a molecularly imprinted polymer sorbent obtained by precipitation polymerization. *Heliyon*. 2019;5(4):e01533. https://doi.org/10.1016/j.heliyon.2019.e01533
59. Pratiwi R, Megantara S, Rahayu D, Pitaloka I, Hasanah AN. Comparison of bulk and precipitation polymerization method of synthesis molecular imprinted solid phase extraction for atenolol using methacrylic acid. *J Young Pharm*. 2018;11(1):12-16. https://doi.org/10.5530/jyp.2019.11.3
60. Hasanah AN, Soni D, Pratiwi R, Rahayu D, Megantara S, Mutakin M. Synthesis of diazepam-imprinted polymers with two functional monomers in chloroform using a bulk polymerization method. *J Chem*. 2020;2020:1-8. https://doi.org/10.1155/2020/7282415
61. Kong Y, Wang N, Ni X, et al. Molecular dynamics simulations of molecularly imprinted polymer approaches to the preparation of selective materials to remove norfloxacin. *J Appl Polym Sci*. 2016;133(1):1-11. https://doi.org/10.1002/app.42817
62. Golker K, Olsson GD, Nicholls IA. The influence of a methyl substituent on molecularly imprinted polymer morphology and recognition—acrylic acid versus methacrylic acid. *Eur Polym J*. 2017;92:137-149. https://doi.org/10.1016/j.eurpolymj.2017.04.043


**How to cite this article:** Suryana S, Mutakin M, Rosandi Y, Hasanah AN. Rational design of salmeterol xinafoate imprinted polymer through computational method: Functional monomer and crosslinker selection. *Polym Adv Technol*. 2022;33(1):221-234. doi:10.1002/pat.5507